A Combined Multiphase Electric Drive and Fast Battery Charger for Electric Vehicles

Topology and Electric Propulsion Efficency Analysis

Luis De Sousa, *Member, IEEE*, Benedicte Silvestre, *Member, IEEE* and Boris Bouchez, *Member,IEEE*

Valeo Engine and Electrical Systems

14, avenue des Béguines, 95800 Cergy Saint-Christophe, France

Email: luis.de-sousa@valeo.com benedicte.silvestre@valeo.com boris.bouchez@valeo.com

***Abstract*— Currently, the main technical weaknesses of Electrical Vehicle (EV) are the limitation of the on-board energy storage and the time to recharge it. Despite of recent improvements in batteries, these drawbacks as well as the cost make the EV not yet attractive. Real challenges for Power Electronics engineers are not only the cost reduction through new system optimizations but also the autonomy increase through the global efficiency improvement and the introduction of a cheap fast on-board charger. This paper deals with a new concept of electric powertrain system which is configurable as a battery charger without additional power components. The interest of this particular solution is the full magnetic decoupling between the rotor and the stator during the charging mode which avoid a clutch system, and prevent the rotor from vibrating. The traction system solution is presented, the feasibility of this combination topology is studied and the effect of the electrical machine's windings configuration is analyzed. Some simulation results show the propulsion efficiency is also improved.**

Keywords- Electric Vehicle, Plug-in Hybrid Vehicle, On-board Battery Charger, 3H-bridge, Power Factor Corrector

I. INTRODUCTION

THE past three years, most of the car makers suffered a strong crisis because of a mismatch between the offer and the increasing demand on the fuel saving and on smaller and cheaper vehicles. The market is achieving a fast trend reversal by proposing a new offer in harmony with sustainable development and with the future environmental laws. Plug-in Hybrid Electric Vehicles (PHEVs) take more advantages of the electric energy by fully charging the battery from the AC grid before each travel. By this way, the battery becomes more cost-effective, more fuel is saved and the carbon oxide emissions are also reduced. This is the reason why the future HEVs cannot get away from an on-board charger. This electronic device is a significant extra cost for HEVs and above all for EVs that need a faster charging and therefore a powerful charger because of its higher battery capacity.

"Cost-killing" policies from automotive part-makers contribute to rethink the EV electric propulsion so that new optimizations and new topologies would be proposed. Using the same expensive components for two or several independent functions should be a successful cost reduction on condition that these functions are not operating in same time in any case. Configuring the electrical machine's coils and the inverter as a battery charger is possible because the battery is charged only when the car is stopped. Not only active and passive power components are saved but also weight and size. This kind of topology is called combination topology in [1] because it uses the drive motor's inverter as a battery charger unlike the independent topology that proposes an independent battery charger. Nevertheless, theses solutions like [4], [5] are suitable for a single-phase charger only. It is interesting to offer a faster charging option by a three-phase plug-in system. Some solutions have been already proposed in [2], [3] but two main drawbacks are recurrent: the first one is the need of a high current relay to connect the AC grid on the electrical machine's coils. This is still an over-cost that makes the solution less attractive. The second one is the generation of magnetic field at the stator which is able to induce high voltage on the rotor's windings or to move it. This is a serious issue in case of Permanent-Magnet Synchronous Machine (PMSM). This paper describes an embedded Three-Phase battery charger without relay that ensures a full magnetic decoupling between the stator and the rotor as described in [6], [7].

In Section I, a brief charger specification is reviewed. The fast charging power target is given. The traction system topology and its performances are compared with the standard ones in Section II, especially in terms silicone surface. In Section III, the configuration of the traction system in battery charger is described and it shows that the charger option does not downgrade the traction system performances. The charging current effect on the electrical machine especially for PMSM is analyzed. In Section V, some simulation results are given to show the efficiency improvements. A validation of the inductance values is also given.

978-1-4244-8218-4/10/$26.00 ©2010 IEEE

II. CHARGER SPECIFICATION

A. Grid Connection

Several considerations about the compatibility must be taken into account in order to propose a vehicle ready to be plugged in any AC grid. The earthing arrangement, the AC plug, the voltage and frequency, the electro-magnetic interference (EMI), the Ground Fault Circuit Interrupter (GFCI), the surge arresters are not tackled in this paper. We focus only on the voltage compatibility and on the low frequency harmonic currents emissions. The battery system is supposed to be always insulated from the chassis and the earth linked to the vehicle's chassis during the battery charging.

According to [8] and to the International Electrotechnical Commission (IEC), we are able to specify an appropriate voltage range compatible with most of the national A.C grids. The Table I shows some examples. We conclude that the charger should withstand nominal phase-to-phase or phase-to-neutral voltages on the range of 100Vac to 430Vac having a frequency on the range of 50Hz to 60Hz. The tolerance is usually of ±10%.

TABLE I. EXAMPLE OF NATIONAL AC GRIDS

Country	Nominal Voltage Single-Phase (LN) / Three-Phase (LL)	Frequency
Australia	240VAC / 415VAC	50Hz
Brazil	110VAC / 380VAC	50Hz-60Hz
China	220VAC / 380VAC	50Hz
France	240VAC / 416VAC	50Hz
Japan	100VAC / 200VAC	50Hz
Russia	220VAC / 380VAC	50Hz
South Africa	220VAC / 430VAC	50Hz
USA	120VAC / 208VAC	60Hz

B. EMC Standards

Non linear loads such as diode rectifiers with capacitive or inductive loads generate harmonic currents which lead to poor power factor. The reactive energy reduces the efficiency of the electricity distribution system. The IEC standards limit these emissions and compel the electric equipments to introduce a system which is able to correct the power factor. The charger must be designed to comply with IEC 1000-3-2 or IEC 1000-3-12 depending on its power rating.

An extensive technical literature deals with the Power Factor correction and with the associated topologies. One of them is interesting for our purpose because of its similarity with a three-phase inverter used to drive an electrical machine. Indeed, the PFC Boost rectifier also called Bridgeless PFC Boost rectifier in [9] has the advantage to simultaneously rectify the alternative current and correct the power factor. Usually, a second stage is useful to step-down the rectified voltage in order to recharge the battery with a suitable voltage level. The figure 1 shows a three-phase charger with PFC.

C. Battery and DC link Voltage Level

The battery nominal voltage depends on the number of cells added in series. One hundred lithium-ion cells are usually found in EV applications because the maximum voltage level of the pack (410V) complies with the 600V IGBT industrial standard. The nominal voltage of this cells arrangement is around 330V. To prevent the cells from a deep discharge, it is recommended not to exceed the minimal threshold (usually higher than 230V). The PFC is based on the Boost topology. This converter rectifies and boosts the voltage from the grid. According to Table I, the PFC output voltage should be designed to withstand at least 750VDC so that the charger is compatible with most of the national ac grid over the world, single phase one as well as three-phase one. The buck converter of the fig.1 defined by S1, S2 and L is required to step down the voltage to an appropriate level for the battery charging.

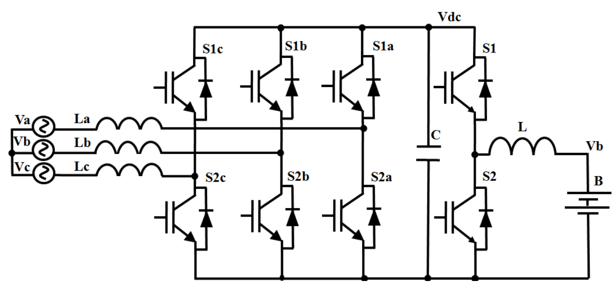

Figure 1. Three-phase Bridgeless Battery Charger (Inverter 1)

D. Fast Charging Power

According to the National Electric Code (NEC), a battery charger supplying more than 14.4 Kilowatts to the battery is a Level 3 charger. Nevertheless, the time to recharge the battery depends on the battery capacity. For the moment, there is no standardization of the "fast charging" definition. Nevertheless, the objective is to provide a combined electric drive and charger able to manage about the same amount of power in both modes: propulsion and battery charging. The topology described in Section IV is able to charge the battery with a high power P_{chg}:

$$P_{chg} = 2\eta \frac{V_{grid}}{\sqrt{3}V_{drive}} P_{drive} \quad (1)$$

where P_{drive} is the maximum continuous power for the motor drive, V_{grid} is the nominal phase-to-phase voltage of the ac grid, V_{drive} the maximum phase-to-phase voltage of the motor drive, and η the efficiency of the power stage. This on-board charger reuses the electronics of the motor drive. The limitation on the charging current is directly linked to the maximum continuous current allowed to supply the machine. In section IV, the charger embodiment is described and it is explained why the maximum current fed by the grid is twice the maximum continuous current tolerable by the electrical machine. An EV equipped with a 545Vac/40KW propulsion system is able to charge the battery with more than 30KW constant power from a 416V Three-Phase power source.

III. Optimal Electric Powertrain Topologies

A. Standard EV architecture

The standard topology is based on a direct DC link between the source of power, usually the battery, and the inverter. The most popular electric motor drive system is a three-phase inverter associated with a wye connected electrical machine. This system has the virtue of simplicity. The neutral avoids zero-sequence currents since the sum of the balanced three-phase currents is null. Each phase is therefore electrically decoupled from each other what is a significant simplification of the control. The main drawback of this architecture is the fact that the battery is directly linked to the inverter. Knowing that the battery has wide voltage range, we guess the optimization of the system is sure difficult. The machine is rated to deliver the maximum torque in the whole battery voltage range but the worst case occurs at the minimum battery voltage. On the other side, the blocking voltage of the switches must withstand the maximum battery voltage. With a scalar command, the maximal current per phase is:

$$I_{MAX} = \frac{2\sqrt{2}w_B}{3\eta\cos\varphi V_{B\min}} T_{q\max} \quad (2)$$

where w_B is the base pulsation at which the phase voltage reaches its maximal value, $cos\varphi$ is the PF, T_q is the torque delivered by the machine and V_{Bmin} the minimum battery voltage.

B. Constant or Adjustable DC link

If we consider an inverter fed by a step-up converter that holds the DC link over the maximum battery voltage, the maximal current becomes lower. The ratio between the two currents is guessed from (2):

$$\frac{I'_{MAX}}{I_{MAX}} = \frac{N}{N'} = \frac{V_{B\min}}{V_{B\max}} \quad (3)$$

This relation is true if the number of turns N of the machine's winding is adjusted according to the voltage ratio. This operation has no impact on the machine dimensions since the magneto-motive force (MMF) is preserved ($N'I'=NI$). Considering a 230V-420V battery voltage range, the Boost converter may reduce the phase current by a factor 1.8 provided that the machine is wound with 1.8 times more turns.

The addition of a step-up Front End Converter (FEC) between the battery and the inverter becomes an opportunity to globally reduce the Silicone Surface Ratio (SSR). Two options are possible since a FEC is available: the DC link is set to the maximum battery voltage (420VDC) or the DC link is set to a much higher voltage (900VDC) even if a new voltage class of IGBT is required. This last option is interesting if the electric drive is foreseen as a battery charger that needs a higher voltage class rated for the ac grid rectification (750VDC). Having a large range between the battery voltage and the DC link offers new opportunities.

The DC link voltage can be adjusted according to the back EMF of the electrical machine to run with a reduced voltage at low speed since the EMF is proportional to the speed. The fig.2 shows the difference between the two options. A significant switching losses reduction is therefore possible above all at low speed. The efficiency at low speed and low torque is critical for energy autonomy considerations. This issue is verified by ARTEMIS Europeans driving cycles.

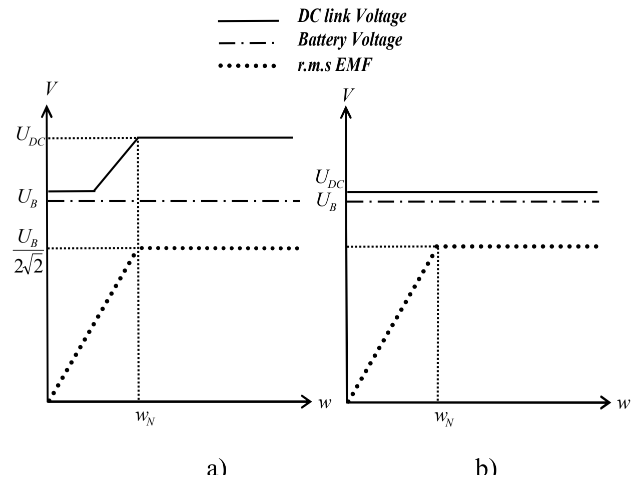

Figure 2. a) adjustable DC link b) Constant DC link

C. 3H-Bridge topology

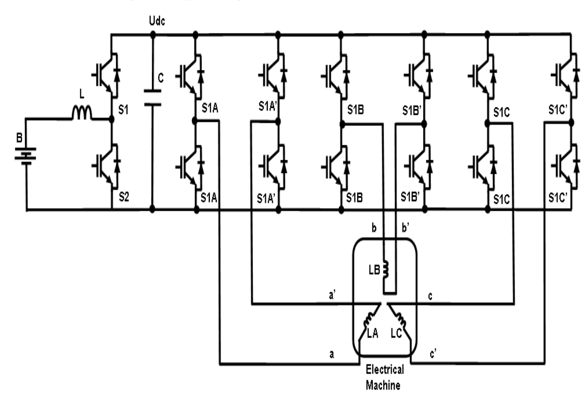

Figure 3. 3H-Bridge Topology (inverter 2)

Another optimization in order to take full advantage of the voltage scale consists of increasing the voltage applied to machine's coils without any IGBT upgrade. This is possible with the H-bridge topology dedicated to each phase. The inverter becomes a set of three H-Bridge (3H-Bridge). Thanks to the 3H-Bridge arrangement, the voltage across a phase is twice compared to the standard inverter of the fig.1. The phase current is reduced to an half but it doubles the number of wires and switches. However, this structure allows switching losses reduction mainly on the turn-on without a *di/dt* increase. Because of the tail current, there is no significant reduction on turn-off. The equivalent frequency seen by the coil is therefore twice the IGBT switching frequency with an appropriated Unipolar PWM. The main drawback of this topology is related to the control. The neutral of a wye connection is useful to cancel the zero-sequence current. From the control point of view, the neutral allows a decoupling of each phase which is usually coupled together by the magnetic circuit of the machine. An open winding connection cannot naturally prevent zero-sequence currents from flowing through each coil and from adding losses and torque ripple. The stator of the machine has to be design with an acceptable zero-sequence inductance. A special care on the zero-sequence current is needful [10].

D. *Silicone Surface Reduction and efficency improvements*

The objective of this section is to compare the SSR of two topologies: the first one is the standard one i.e an inverter directly fed by the battery (inverter 1), the second one is a 3H-Bridge inverter fed by a Boost type FEC (inverter 2). We consider that the DC link voltage is a factor of the maximal battery voltage, 840V for example. We consider that the cooling system that drains the heat from the die to the ambient is the same for both cases. The power losses densities of each solution are considered equal for both solutions. Comparing the surfaces becomes easy: the SSR between the two inverters (S_{Inv1} to S_{Inv2}) is in fact the total silicone power losses ratio. Of course, the FEC that generates the high voltage networks has to be added in the silicon surface balance (S_{FEC}). We consider the FEC meets the same limitation on the *di/dt* and power losses density. This calculation is done with ideal switching waveforms (no tail current). The theoretical calculation is done for the worst case of each converter: locked rotor for the inverter, maximal power for the FEC. The result is generalized with this formula:

$$\frac{S_{FEC}+S_{Inv2}}{S_{Inv1}} \approx \frac{1}{1+R_1}\left(\frac{V_{DC}}{4\eta V_{B\max}}R_1+\frac{1}{8\eta^2}+\frac{V_{B\min}}{V_{B\max}}R_1+\frac{1}{4}\left(\frac{V_{B\min}}{V_{DC}}\right)^2\right) \qquad (4)$$

where R_1 is the conduction to switching losses ratio of the first inverter, V_{DC} the maximal DC link and η is the FEC efficiency. The size reduction is drastic. For example, we compare a first 600V inverter with balanced losses (i.e R_1=1) fed by a 230V-410V battery pack with a second 1200V inverter fed by a Hard Switching FEC (η=90%). About 38% of SSR should be saved.

This formula shows that the 840V DC link is not an optimum. This is due to the FEC and the Hard Switching mode. Whatever the DC link voltage level, the battery current is invariant so the switching losses due to the FEC are increased with the DC link voltage. A 410DC link is optimal but it is not compatible with three-phase battery charging. Nevertheless, the silicon surface saving is noticeable and it is reduced with a Soft Switching FEC. The propulsion efficiency is also higher. The electrical machine keeps about the same losses for both solutions. The hypothesis of an invariant MMF means an invariant current density (same filling ratio, same winding area) and an invariant flux variation per turns. The copper losses and the Eddy currents losses are therefore unchanged. These results are checked in Section V with accurate calculation based on Power Modules datasheets.

IV. COMBINED BATTERY CHARGER & ELECTRIC DRIVE

A. *Inverter Configuration as Battery Charger*

The fig.4 shows how the proposed topology can be configured as a high power charger. The three-phase grid is connected to the mid-point a_o, b_o, c_o of each machine's coils through a small EMI filters and other protections. No relay is necessary. The ac plug and the filters do not disturb the system during propulsion mode. It would be possible to connect the grid to the extremities *a*, *b*, *c* or *a'*, *b'*, *c'* but the charging three-phase currents generate a rotating magnetic field at the stator level. Depending on the type of rotor, this magnetic field may be annoying. The induction machine rotor may moved by induction. In case of wound rotor, even if the excitation is turned off, current can flow through the freewheeling diodes of excitation. In case of permanent magnet, rotation, vibration is also possible.

A better solution is to access to the mid points of each phase so that the ac grid is connected to them during the charging mode. Then, each leg of the same bridge drives the current of split-phase to be equal and in phase with the 50Hz or 60Hz input voltage. The ac current is therefore rectified to source the DC link. Then, the FEC operates in reverse mode i.e in buck mode in order to recharge the battery with a suitable current and voltage. Another advantage of this embedded bridgeless PFC is the suppression of the “cups effect”.

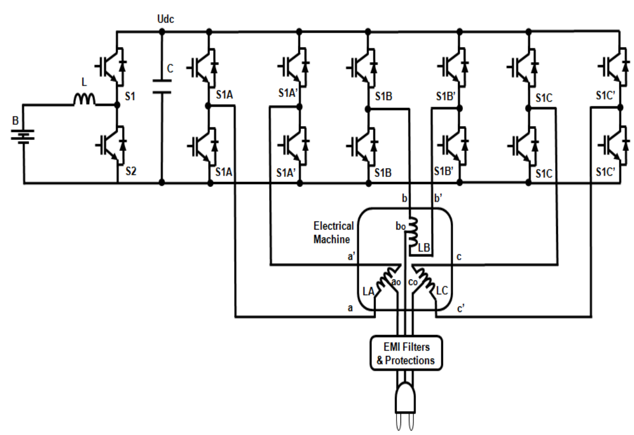

Figure 4. Embbeded Charger

B. *Rotor to Stator Magnetic decoupling*

The fact the grid is connected to the mid-points of each phase makes the currents coming from the grid to be split in two opposite and equal currents. On the whole stator, the MMF is cancelled because the current of one split-phase coils destroy the effect of the other one. This cancellation ensures a magnetic decoupling between the rotor and the stator. No rotation or large displacement of the rotor is possible even if permanent magnets are mounted. Some slight vibrations are still possible because of an unbalanced rotor mass or an unbalanced current sharing.

C. *Magnetic flux distribution along the air gap*

If the MMF is locally cancelled, in the same slot for example, the apparent inductance in charging mode is therefore similar to the leakage inductance which is too low for a proper charger operation. To avoid such a disagreement, a special winding arrangement is necessary. A basic solution is to wound the coil in several slots at least two of them. A soft distributed winding creates a common mode inductance between the midpoint of the phase and the phase terminals. The numbers of slots, of poles and the winding arrangement have important consequences in the machine behavior during the charging mode, especially on the vibrations.

To demonstrate the feasibility of this kind of embodiment, we consider an example of machine that are seldom used but it simplicity allows a didactic approach without hard calculation. A PMSM has 4 poles, 24 slots and no saliency L_s=L_d). The poles are connected in parallel. This arrangement cancels the MMF every two slots as described in fig.5. The flux distribution along the air gap is then homogeneous and similar to which ones encountered during the normal operation of the machine.

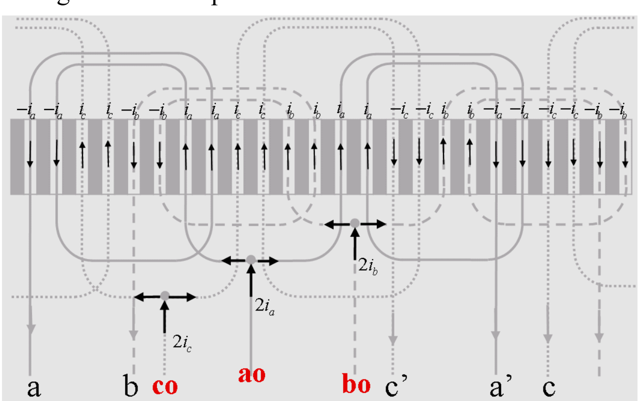

Figure 5. Windings arrangement for poles parralleling

V. SIMULATION RESULTS

A. *Size reduction*

The comparison is done with two solutions. A machine and an inverter are designed based on real components available on the market. The first one is a standard solution. A 40KW/60KWpeak PMSM controlled by a 600V inverter directly linked to a 240V-420V Battery. The second one is the same machine but wound with 3.5 times more turns and controlled by a 1200V 3H-Bridge inverter. This inverter is fed by a bi-directional boost converter 240V-900V. The Boost is made of three interleaved cells in hard switching mode. The switching frequency of both inverters is set to 12Khz. Note that the maximum current to be withstand by the first inverter is 540Apeak per phase. This current appears when the rotor is locked. The second inverter is rated only for 71Apeak thanks to the topology and the adjustable DC link. The table III confirms the expected reduction of SSR. The results of the diode are about the same.

TABLE II. SILICONE SURFACE COMPARISON

	Solution n°1 ***600V***	**Solution n°2** ***1200V***		
	Standard Inverter	*FEC* *Hard Switching*	*FEC* *Soft Switching*	*3H-Bridge*
IGBT die Part Number (Infineon)	6 X 8 SIGC100T60R3 (200A)	6 X 2 SIGC158T120R3 (150A)	12 X 1 SIGC84T120R3 (75A)	6 X 1 SIGC84T120R3 (75A)
IGBT die	796mm²	158mm²	84mm²	84mm²
Total Surface	4776mm²	2908mm²	2016mm²	1008mm²
Surface Reduction	-	-39%	-58%	-

The reduction seems amazing but it is explained by the fact that the IGBT switching speed of the first inverter must be slow down to not overlap 2000A/µs. Moreover, the current to be switched is about 8 times higher than the propose solution. Another significant optimization is the DC link reduction when the rotor is locked.

B. *Powertrain Efficiency*

It is interesting to compare the efficiency of both solutions according to a realistic average driving cycles such as ARTEMIS ones. The Fig.6 plots the distribution of the E.M torque and speed along several cycles.

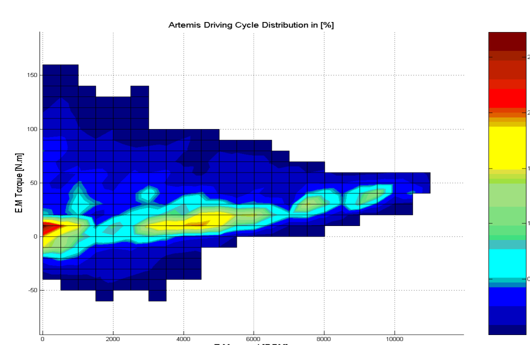

Figure 6. Mixed Mission Profil

Note that the E.M is rarely used at peak power. This analysis confirms that the powertrain must be improved at low power and low speed in order to increase the autonomy of the vehicle. The new topology allows a significant reduction of losses also at high power. More than 2KW are saved during a huge vehicle take-off. More than 1KW are saved on highway. The Fig.7 shows the power saved thanks to the proposed topology is at least few hundred of watts. The Fig.8 shows the benefits of the Soft Switching FEC. The power saving is higher for any operating points.

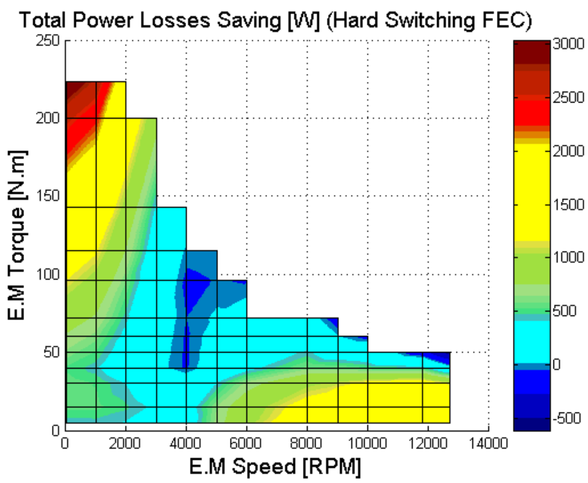

Figure 7. Power saved thanks to the new topology (Hard Swithing)

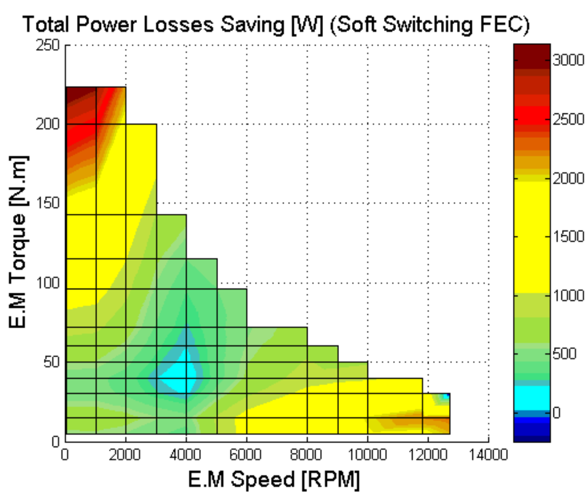

Figure 8. Power saved thanks to the new topology (Soft Switching)

C. *Flux distribution*

A 4 poles machine with two 24 slots is built for simulation. The air gap height is not realistic but it is helpful for clarify the drawing. A two dimensions Finite Element simulation was performed with FEMM. The Fig.9 shows that the flux is homogeneously distributed along the air gap. The simulation has allowed a verification of the self and mutual inductances of each split-phase by measuring the flux of each semi coils. The low coupling of the coils in charging mode is confirmed.

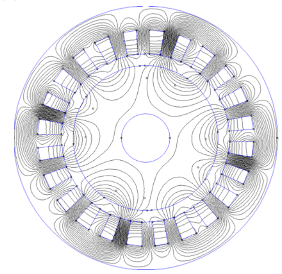

Figure 9. E.M in battery charging mode (poles in parallel)

VI. CONCLUSION

The following paper deals with a new topology that is optimized for a full electric drive. The electrical system is based on a Boost type FEC and a 3H-Bridge inverter. This architecture allows a significant 39% of silicone saving. Despite of the FEC, the global efficiency of the new topology is better even if the DC link is set to 840V. A constant DC link of 420V is optimal but not compatible with the three-phase battery charger function. This particular topology allows to plug the vehicle into the grid through the midpoints of the machine's winding. The charger is therefore combined with the electric drive. The effect of the charging on the machine was analyzed and not calls into question the feasibility of the proposed solution.

VII. REFERENCES

[1] L. Shi, A. Meintz, M. Ferdowski, "Single-Phase Bidirectional AC-DC Converters for Plug-in Hybrid Electric Vehicle Applications", *IEEE Vehicle Power and Propulsion Conference (VPPC08),* Harbin, China, Sept. 2008

[2] C. Stancu, S. Hiti, E. Mundt, "Modile Electric Power for Medium and Heavy Duty Hybrid Electric Vehicles", *35th IEEE Power Electronics Specialists Conference (PESC04)*, Aachen, Germany, 2004

[3] Kinoshita Shigenori, "Electric System for Electric Vehicle", Japanese patent JP6276615, Fuji Electric Co LTD, Sept. 30, 1994

[4] L. Solero, "Nonconventional on-board Charger for Electric Vehicle Propulsion Batteries", *IEEE Trans. on Vehicular Technology*, Vol. 50, NO. 1, Jan. 2001

[5] S-K. Sul, S-J. Lee, "An Integral Battery Charger for Four-Wheel Drive Electric Vehicle", IEEE Trans. on Industry Applications, Vol. 31, NO. 5, Sept. 1995

[6] L. De-Sousa, B. Bouchez, "Combined Electric Device for Powering and Charging", International Patent WO 2010/057892 A1

[7] L. De-Sousa, B. Bouchez, "Method and Electric Combined Device for Powering and Charging with Compensation Means", International Patent WO 2010/057893 A1

[8] U.S Departement of Commerce International Trade Administration, "Electric Current Abroad", 1998 edition, reprinted Feb. 2002

[9] G. Chen, K.M. Smedley, "Steady-State and Dynamic Study of One-Cycle-Controlled Three-Phase Power-Factor Correction",IEEE Trans. on Industrial Electronics,Vol.52, NO.2, April 2005

[10] Y. Crévits, X. Kestelyn, E. Semail, "Investigation on Vector Control of Three-Phase Synchronous Machines Under Supply Fault Conditions", Power Electronics, Electrical Drives, Automation and Motion, SPEEDAM 2006, International Symposium on, pp. 439-444, Taormina, Italy, May. 2006